Reaction Kinetics, Mechanisms and Catalysis
https://doi.org/10.1007/s11144-018-1522-x

Protection of industrially-relevant Pd/C catalysts for cyclohexene hydrogenation: effect of a siliceous coating on the thermal treatment of covered catalysts

Vincent Dubois[1] · Didier Desmecht[1] · Laylla Rkiouak[1] · Anne-Sophie Jacquet[1] · Tomoya Hoshinoo[2] · Keizo Nakagawa[2,3] · Sophie Hermans[4]

Received: 22 October 2018 / Accepted: 8 December 2018

Abstract

Carbon-supported palladium catalysts were covered by a siliceous layer to increase their sintering resistance. A commercial Pd/C catalyst was compared to catalysts prepared either by dry impregnation or wet impregnation on activated carbon or carbon black. In the case of dry impregnation, the Pd active phase was shown to be located within the micropores of the carbon support. A smooth and thick siliceous layer was evidenced by electron microscopy. XPS showed that Pd was indeed covered by a layer containing Si atoms. In all cases, the catalytic activity was diminished by the presence of the protecting layer, but thermal treatment allowed increasing the activity by creating some porosity within the layer, therefore allowing access to the underlying active phase, without deleterious sintering. Carbon black proved its superiority thanks to its non-microporous nature, which allowed the Pd particles to be located at the interface with the siliceous coating hence making them more accessible.

Keywords Palladium · Carbon · Silica · Protection · Sintering · Deactivation

✉ Sophie Hermans
Sophie.Hermans@uclouvain.be

[1] Laboratoire de Chimie Physique et Catalyse, LABIRIS, Avenue Emile Gryzon 1, 1070 Brussels, Belgium

[2] Department of Advanced Materials, Institute of Technology and Science, Tokushima University, 2-1 Minamijosanjimacho, Tokushima 770-8506, Japan

[3] Division of Advanced Membrane Science and Technology, Graduate School of Science, Technology and Inovation, Kobe University, 1-1 Rokkodai, Nada, Kobe 657-8501, Japan

[4] Institute of Condensed Matter and Nanosciences (IMCN), Université catholique de Louvain, Place Louis Pasteur 1, 1348 Louvain-la-Neuve, Belgium

Published online: 01 January 2019

Introduction

Metallic nanoparticles supported on carbon or oxides have proven their usefulness as heterogeneous catalysts for many reactions. In particular, noble metals such as palladium are ubiquitous, and have been applied mainly for hydrogenation reactions [1]. More recently, Pd heterogeneous catalysts have been shown to catalyze C–C bonds formation (Suzuki, Heck and associated) and can therefore be used for fine chemicals syntheses [2]. In both cases, carbon supports are often selected due to their availability and stability. The preparation of carbon-supported Pd catalysts can be carried out using several methods including deposition–precipitation, impregnation and ion-exchange [3]. Over the years, we have developed original methods for Pd/C catalysts syntheses, based on maximizing metal precursor/support surface interactions [4–9].

These Pd supported catalysts are commonly used in the industry but suffer from deactivation. Stability of heterogeneous catalysts is of major industrial relevance, especially in the case of costly noble metals. Deactivation might arise from thermal, mechanical or chemical causes [10–16]. Supported catalyst deactivation occurs via different phenomena, among which active phase leaching, sintering or poisoning are the most important [10–16]. In particular, the deactivation of Pd catalysts has been studied [17] but many questions remain on the industrial scale. Engineering solutions against deactivation exist, such as tailored reactors and process design [18], but they will merely retard the onset of deactivation without completely suppressing it. In the case of biomass valorization in particular, much research is still needed to mitigate the fouling, poisoning, and destruction of the catalyst, because traditional petrochemical supports do not survive the hydrothermal and often acidic conditions applied in biomass conversion processes [19]. Carbon is therefore an interesting alternative support.

Sintering may be avoided by covering the catalyst by a protective layer. However, a major challenge in this approach is to optimize the overlayer thickness and porosity in order to maintain activity while conferring increased stability. Leaching is most often due to corrosion mechanisms leading to ionic species that diffuse in the liquid phase. Covering might also slow down this process [20] because soluble species will be less easily washed off and might even get trapped in the protecting layer, especially when it is polar and/or presents surface charges.

The covering approach has been demonstrated by various authors over recent years, mainly for platinum-based catalysts. For example, Pt nanoparticles deposited on SiO_2 spheres were encapsulated by either mesoporous SiO_2 or TiO_2 shells and used in hexane reforming [21]. The cover shells were shown to hinder Pt sintering. Another system based on Pt nanoparticles supported on TiO_2 nanofibers was prepared by deposition of PVP-stabilized Pt nanoparticles onto the TiO_2 surface, then the formation of a SiO_2 coating by the Stöber method followed by calcination [22]. The sample was compared to Pt/TiO_2 nanofibers without SiO_2 coating and shown to resist sintering up to a temperature of 750 °C in air. Another approach consisted of coating pre-formed Pt_3Co_1 nanoparticles by a protective siliceous layer before adsorption on carbon black support [23]. An embedded 1 wt% $Rh@Al_2O_3$ catalyst,

composed of Rh nanoparticles embedded in an Al_2O_3 matrix and stable at high temperature, was prepared by the precipitation of $Al(OH)_3$ in the presence of stabilized Rh nanoparticles, followed by calcination [24]. In this case, the protecting layer is not added in a subsequent step. Palladium nanoparticles embedded in the inner surfaces of carbon nanotubes were also demonstrated to be sinter-resistant and highly recyclable [25]. Pt nanoparticles located in the inner cavities of mesoporous silica hollow spheres were developed as an alternative possessing high sintering resistance [26]. Pd@hCeO_2 hollow core–shell nanocomposites composed of Pd nanoparticles encapsulated within CeO_2 hollow shells were reported as well [27]. A recent study reports protection by embedding Pd catalysts into poly(dimethylsiloxane) (PDMS) layers [28]. Studies on the regeneration of Pd/C catalysts have also appeared [29].

Our previous work on platinum supported on carbon black showed the ability of siliceous cover layers to protect the catalyst while preserving some activity in cyclohexane dehydrogenation into cyclohexene [30–34]. The protecting layer is formed by hydrolysis and condensation of organosilanes such as tetraethoxysilane (TEOS) and aminopropyltriethoxysilane (APTEOS). The latter compound is used to favor interactions with the starting denuded surface. In the case of carbon supports, one might expect the formation of surface amide bonds between the NH_2 groups of APTEOS and oxygenated surface functions.

Here we study the covering of carbon-supported palladium catalysts applied in the hydrogenation of cyclohexene into cyclohexane. The goal is to use this transformation as test-reaction but not to optimize it. This reaction is more demanding than dehydrogenation, as it requires the simultaneous presence of two reactants (cyclohexene and hydrogen) at the active site. We compare activated carbon with carbon black to evaluate the impact of the support porosity in this context. We also compare wet impregnation (WI) with dry impregnation (DI) also commonly named incipient wetness, because the active phase will not be similarly located on the support using both methods. The effect of various heat treatments on the catalysts characteristics (textural properties, metal dispersion) and catalytic activity is described.

Our goal is to show that a compromise must be found between protection ability of a covering layer and accessibility of the underlying active phase. Therefore, the experimental protocol involves batch experiments to compare the activity of the fresh covered catalysts and to rank these catalysts by comparison of their activities in the target reaction. The challenge is to master the balance between efficient catalyst coverage while keeping the access to the active sites.

Experimental

Syntheses

A commercial 5% palladium on activated carbon catalyst from Johnson Matthey (5% Pd/C type 440) was used as reference. It is noted JM440, and JM440-*value* when heat-treated (the '*value*' being the highest temperature reached during thermal treatment).

Pd catalysts supported on activated carbon (Pd/C) were prepared from the DARCO G60 (Produced by Norit from lignin and distributed by Fluka; abbreviated DG60) support by either dry impregnation (DI) or wet impregnation (WI) [35]. For comparison, another microporous activated carbon from Norit was also used (Norit SX Plus, noted SX+). In the first case (DI), 0.6 mL of an aqueous solution containing 0.083 g_{Pd}/mL prepared from H_2PdCl_4 was added to 1 g support. After mixing, the catalyst is dried under nitrogen (30 mL/min) at 130 °C for 2 h followed by reduction under hydrogen (30 mL/min) at 200 °C for 1 h, and further heating under nitrogen (30 mL/min) at 200 °C for 1 h. In the second case (WI), 1 g support was poured in 100 mL aqueous solution containing H_2PdCl_4 (0.05 or 0.02 g_{Pd}). After 1 h of stirring, the absence of metal remaining in solution was verified by ICP-OES (PerkinElmer Optima RL3300). Drying and reduction were carried out as described above for DI. These catalysts are noted *XXn-support*, where *XX* is either WI or DI (preparation method) and *n* is the Pd loading (2 or 5%).

The covering of the catalysts prepared by either DI or WI, as well as JM440, by siliceous layers was carried out from aminopropyltriethoxysilane and tetraethoxysilane (TEOS) as follows. 1 g of reduced catalyst was dispersed in 220 mL water and sonicated for 5 min. The pH was adjusted at 10 by addition of triethylamine. Successive hydrolysis of 3-aminopropyltriethoxysilane at 60 °C for 30 min and tetraethoxysilane at 60 °C for 1 h led to siliceous coating formation. The solid sample was recuperated by centrifugation, dried at 60 °C in air and reduced under hydrogen at either 200 or 400 °C.

The covered catalysts are noted *Si@XXn-support*.

A covered Pd/CB (CB = carbon black, Vulcan XC-72 from Cabot Co) catalyst was also prepared in one step by the following method. The coverage of Pd/CB with siliceous layers was performed by the successive hydrolysis of APTES and TEOS. CB was immersed in an aqueous solution containing H_2PdCl_4. The pH of the solution was adjusted to 10 by the addition of triethylamine, and the Pd metal precursors were then deposited onto the CB surfaces. After this solution was filtered, the sample was dispersed in an aqueous solution containing triethylamine (pH 10). APTES was added to the solution, and the solution was stirred at 60 °C for 30 min. TEOS was then added to the solution and stirred at 60 °C for 1 h. After centrifuging and drying at 60 °C, the samples were exposed to H_2 atmosphere at either 200, 400 or 800 °C. Hereafter, the obtained samples are noted *SiCB7wt*.

Instrumental

The catalysts thermal treatments were performed in a Carbolite MTF12/38/250 vertical oven, coupled to a temperature controller Eurotherm 91. The sample was introduced in a metallic tube then heated to 130 °C for 1 h under nitrogen. It was then swept by a hydrogen flux and the temperature was increased at a rate of 20 °C/min to reach the desired value. The working temperature was maintained for 1 h before cooling under nitrogen.

The nitrogen adsorption isotherms were carried out on a *Gemini VII* instrument from Micromeritics at 77 K. The sample (70 mg) was dried at 150 °C

under nitrogen for 30 min and then degassed under 20 µmHg prior analysis. The specific surface area (m^2/g) was calculated from the adsorption data using the Brunauer–Emmet–Teller (BET) method. The mean pore diameter was determined using the BJH method. Total pore volume was determined by a single point adsorption measurement at a relative pressure of 0.98. The microporous volume was determined by the de Boer's t-plot method. The relative errors are 1 to 7% on BET specific surface area values; 3% on total pore volume values; 4 to 7% on microporous volume values and about 10% on mean pore diameter values.

Metallic dispersion measurements were conducted by CO chemisorption with a *Pulse Chemisorb 2700* apparatus from Micromeritics [36]. The sample (about 50 mg) was first reduced under a hydrogen flow at 150 °C during 1 h. Then, it was swept by a helium flow at 200 °C for 2 h. The sample was finally brought back to room temperature at which time it was subjected to a sequence of CO pulses. The metallic dispersion was calculated from the cumulative amount of adsorbed CO (i.e. the sum of non-detected CO in each pulse), following:

$$D = \frac{V_{NTP} \cdot M}{V_M \cdot m \cdot C \cdot P} \times 100$$

Here D is the metallic dispersion (%), V_{NTP} is the adsorbed volume under normal temperature and pressure conditions, M is the atomic weight of the metal (here, Pd), V_M is the molar volume (22.414 L/mol) of the active gas at normal conditions (0 °C, 1 atm), m is the dry sample mass, C is the stoichiometric coefficient for CO adsorption on Pd (a 1:1 stoichiometry was considered in the present study [37–39]) and P is the wt% of metal in the sample. The absolute mean error on dispersion values is 1%.

Scanning electron microscopy (SEM) images were obtained on a FEG Digital Scanning Microscope (*LEO DSM 982 Gemini* from Carl Zeiss Cie), equipped with an EDAX detector (Phoenix CDU LEAP). The samples were fixed by double-face conductive carbon sticky tape on 5 mm diameter Al specimen stubs (Agar Scientific).

Transmission electron microscopy (TEM) images were obtained on a *LEO 922 OMEGA Energy Filter* Transmission Electron Microscope operating at 200 kV. The solid samples were suspended in ether under ultrasounds. On drop of supernatant containing the smallest particles was then deposited on a holey carbon film supported on a copper grid, before being dried at 30 °C for 2 h under vacuum.

X-ray photoelectron spectroscopy (XPS) was carried out at room temperature on a *SSI-X-probe (SSX-100/206)* spectrometer from Fisons connected to a computer running the S-probe software. The samples were fixed by double-face isolating sticky tape on small brass troughs and placed on a ceramic rotating sample holder (Macor® Switzerland), capped by a Ni grid on a 3 mm O-ring to avoid charge effects. During analysis, the created surface charges were neutralized by a floodgun of energy fixed at 8 eV. The pressure in the analysis compartment was 10^{-6} Pa. The data were interpreted with the CasaXPS software. The photopeaks were calibrated with reference to the C–C,H component which was fixed at 284.8 eV. The peaks were decomposed into a sum of Gaussian/Lorentzian (85/15) after subtraction of

a Shirley baseline. Constraints were used for decomposing the Pd3d peak: area ratio (Pd3d5/2/Pd3d3/2) = 1.5, difference in energy Pd3d3/2 − Pd3d5/2 = 5.26, FWHM = 1. A first doublet appears at Pd3d5/2 = 335 eV (Pd^0), while the second is 3 eV further for Pd^{II}.

The GC chromatograph was an *Agilent Technologies 6890 N*. Two WCOT fused silica columns from *Chrompack* were used indistinctly to perform the analysis of the reaction medium: *CP-WAX 52 CB* capillary column (50 m × 0.53 mm ID, 2 µm film) and *CP-Sil 8 CB* capillary column (25 m × 0.32 mm ID, 5 µm film). The vector gas was He (50 kPa) and the temperature of the injector and detector was kept at 250 °C. The samples were automatically injected via a split–splitless injector with a split flow of 20 mL/min. The temperature program for analysis, using the *CP-WAX 52 CB* column was as follows: 50 °C for 5 min, heating to 150 °C (20 °C/min), isotherm at 150 °C for 1 min. The temperature program with the *CP-Sil 8 CB* column consisted in an isotherm at 100 °C for 1 min, then a first heating to 150 °C (10 °C/min) and a final heating to 200 °C (25 °C/min). The signal received by a FID detector was directly interpreted by a computer using the HP Chemstation software. The surface area of each peak was converted into concentration by applying the response factor with respect to the internal standard.

Catalytic tests

The catalytic tests for cyclohexene hydrogenation into cyclohexane were carried out in a 1 L steel *Parr 4521* batch reactor fitted with a temperature control device *Parr 4842* and a mechanical stirrer fixed at 1700 rpm. Standard tests have been performed to ensure kinetic regime and to avoid extra-granular diffusion limitation. 350 mL methanol (Chemlab, puriss. > 99.7%), a known quantity of catalyst (depending on the Si content and the availability, the involved quantity corresponds to 2.5 to 6 mg of Pd in each test) and 8 mL n-octane (chromatographic internal standard, Janssen Chimica, p.a. > 99%) were poured in the reactor and degassed (15 min) under nitrogen. A pretreatment was applied to the catalyst at 40 °C for 1 h, under 5 bar of H_2. 25 mL cyclohexene (Chemlab, pur. > 99%) and 25 mL degassed methanol were then added in the reactor under N_2. During catalytic reaction, the reactor was kept under a pressure of ~ 2 bar H_2 and a temperature of 21 °C. Aliquots of the reaction mixture were taken at regular time intervals and analyzed by gas chromatography (GC). At the end of the test, the catalyst was separated from the reaction mixture by filtration.

Pseudo-zeroth order was considered for the kinetics involving uncovered catalysts, as the linear trends were observed for conversion rates as high as 70 to 90%. Thus, the specific activity is determined by the slope of the linear part of the reactant or product concentration versus time curve. In the case of the covered catalysts SiCB7wt, the specific activity is also determined by the slope of the linear part of the C,t plot, as the pseudo zero-order kinetics can be considered for conversion rates ranging from 45 to 50%. In the case of covered catalysts based on activated carbon (JM440, DG60 and SX+), the kinetics cannot be fully interpreted as a zero-order reaction. Nevertheless, it exhibits a linear trend during a large part of the reaction (between 10 and 65–90% of conversion). In order to compare the results easily with their uncovered counterparts, a

kinetic constant was determined for this pseudo-zeroth order reaction. No side product was observed. The results are normalized with respect to the mass of catalyst or Pd introduced. The catalytic activity is thus expressed in M min^{-1} $g^{-1}_{(Pd)}$. The relative errors on specific catalytic constants are about 10%.

Results and discussion

Study of commercial catalyst

Investigation of sintering

A JM440 commercial catalyst was first heated to several temperatures and characterized, to study the impact of thermal treatment on the type of catalyst studied here. Results show a strong effect on metal dispersion measured by CO chemisorption but no major modification in textural properties (Table 1). Indeed, Pd dispersion decreased dramatically when increasing the temperature above 200 °C, while surface and pores characteristics remain constant. Accordingly, the hydrogenation activity diminished when increasing the heat-treatment (Fig. 1). Moreover, the linearity of the kinetic plot was lost earlier (it was linear up to 90% conversion with the catalyst without thermal treatment, while it reduces to 65% conversion for the sample heated at 400 °C).

Covering of commercial catalyst

The JM440 commercial catalyst was then covered by a protecting siliceous layer and similarly submitted to thermal treatments at different temperatures. The textural properties of this series of materials are given in Table 2. It was found that the covering layer suppresses access to the carbon support porosity, hence lowering specific surface area and porous volume. However, when treating thermally, some porosity is re-created within the protecting layer. If the siliceous layer is thinner (noted 1/4Si, last line of Table 2), more surface and pore volume remain available. SEM imaging of the protected catalysts showed the grains covered by a smooth siliceous layer (Fig. 2b), in strong contrast with the starting sample (Fig. 2a). At the highest temperature treatments, cracks were visible within the coating (Fig. 2b). The covered catalysts remained active in hydrogenation. The activity in this case increased with the treatment temperature (Table 2), in accord with restoration of some porosity when heating. This demonstrates the effectiveness of the siliceous layer to counteract deactivation by sintering. The catalyst covered by a thinner layer is the most active in line with its textural properties (noted 1/4Si, last line of Table 2).

Table 1 Characterization of JM440 (Pd/C 5%) commercial catalyst thermally treated (at 200–800 °C)

Sample	Thermal treatment	Specific surface area (m^2/g)	Total pore volume (cm^3/g)	Microporous volume (cm^3/g)	Mean pore diameter (Å)	Metallic Pd dispersion (%)	Specific kinetic constant k′ ($M\ min^{-1}\ g_{Pd}^{-1}$)
JM440	None	748	0.543	0.174	29	13	2.28
JM440-200	200 °C	849	0.607	0.203	29	14	0.81
JM440-400	400 °C	838	0.608	0.198	29	8	0.34
JM440-600	600 °C	868	0.645	0.201	30	2	0.03
JM440-800	800 °C	862	0.646	0.197	30	< 1	n.d.

The cyclohexene hydrogenation activity of the thermally treated JM440 catalysts is quantified by the specific kinetic constant k′ (solvent = methanol, initial concentration in cyclohexene = 0.6 M, total volume = 0.4 L, m_{Pd} = 4 mg, P_{H_2} = 2 bar, T = 21 °C)

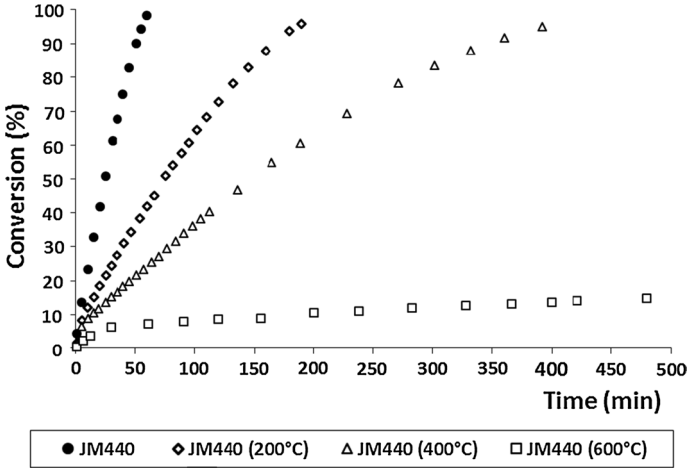

Fig. 1 Cyclohexene conversion versus time for the commercial catalyst JM440 (Pd/C 5%) and the JM440 catalyst thermally treated at 200, 400 and 600 °C (reaction conditions: solvent = methanol, initial concentration in cyclohexene = 0.6 M, total volume = 0.4 L, m_{Pd} = 4 mg, P_{H_2} = 2 bar, T = 21 °C)

Table 2 Characterization of protected JM440 catalysts treated at different temperatures (200–800 °C)

Sample	Specific surface area (m^2/g)	Total pore volume (cm^3/g)	Microporous volume (cm^3/g)	Mean pore diameter (Å)	Specific kinetic constant k′ ($M\ min^{-1}\ g_{Pd}^{-1}$)
½Si@JM440-200	41	0.042	0.003	41	1.43×10^{-3}
½Si@JM440-400	36	0.040	0.002	45	1.12×10^{-3}
½Si@JM440-600	112	0.078	0.026	28	2.20×10^{-3}
½Si@JM440-800	166	0.114	0.038	28	3.45×10^{-3}
¼Si@JM440-800	289	0.175	0.082	24	5.74×10^{-3}

The cyclohexene hydrogenation activity of the different protected JM440 catalysts is quantified by the specific kinetic constant k′ (solvent = methanol, initial concentration in cyclohexene = 0.6 M, total volume = 0.4 L, m_{Pd} = 2.5 mg for 1/4Si and 6 mg for 1/2Si, P_{H_2} = 2 bar, T = 21 °C)

Investigation of palladium on activated carbon catalysts

Influence of the preparation method

Catalysts supported on activated carbon were prepared with DG60 support by either dry impregnation (DI) or wet impregnation (WI). This activated carbon support is highly microporous (Table 3). The Pd/C catalysts prepared by dry impregnation display a lowering of specific surface area and porosity compared to starting support, while no major change is observed in the case of wet impregnation (Table 3). This shows that dry impregnation allows penetration of the active phase deeper into the pore structure, blocking some micropores hence reducing internal surface

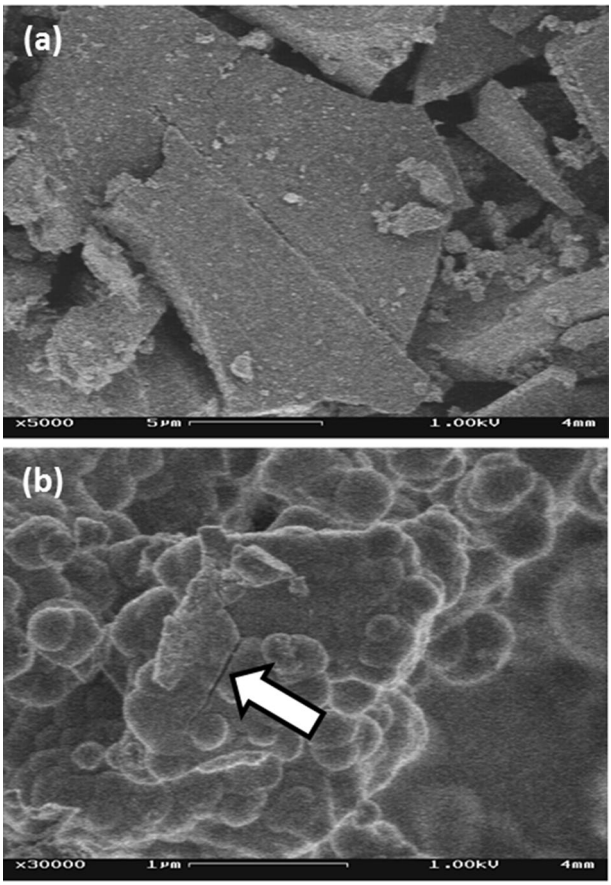

Fig. 2 SEM images of the JM440 catalyst treated at 800 °C **a** uncovered, **b** coated by a 1/2Si layer (crack marked by arrow)

Table 3 Textural characteristics of catalysts supported on DARCO G60, prepared by dry impregnation (DI) or wet impregnation (WI)

Sample	Specific surface area (m^2/g)	Total pore volume (cm^3/g)	Microporous volume (cm^3/g)	Mean pore diameter (Å)
Darco G60	954	0.624	0.252	40
DI5-DG60	798	0.579	0.202	45
WI5-DG60	909	0.616	0.248	43
WI2-DG60	944	0.632	0.258	42

area. These catalysts were also characterized by XPS (Table 4). The Pd surface concentration is much higher on the commercial than synthesized catalysts. Amongst those latter materials, the catalysts prepared by dry impregnation present the lowest Pd content values, confirming that the active phase is located within the pores.

Table 4 XPS characterization of catalysts supported on DARCO G60 and SX+ supports, prepared by dry impregnation (DI) or wet impregnation (WI) and specific activity of catalysts prepared on DARCO G60 and SX+ supports in the hydrogenation of cyclohexene (solvent = methanol, initial concentration in cyclohexene = 0.6 M, total volume = 0.4 L, m_{Pd} = 4 mg, P_{H_2} = 2 bar, T = 21 °C)

Sample	C (%)	O (%)	Pd (%)	Pd/C (%)	Pd(II)/Pd(0) (%)	Specific kinetic constant (M min^{-1} g_{Pd}^{-1})
SX+	96.10	3.90	–	–	–	
DG60	94.51	5.49	–	–	–	
JM440	69.06	22.25	7.34	0.106	1.92	
WI5-SX+	94.72	4.41	0.86	0.009	0.83	0.7
WI2-SX+	95.82	3.80	0.38	0.004	1.19	0.7
DI5-SX+	93.76	5.63	0.43	0.005	0.60	0.6
DI5-DG60	94.18	4.61	0.43	0.005	n.a.	1.2
WI5-DG60						1.0
WI2-DG60						1.2

Expectedly, when the loading decreases, the Pd surface atomic% also decreases. All catalysts present a mixture of Pd(II) and Pd(0) at their surface, with the commercial catalysts being characterized by the highest Pd(II) proportion in correlation with higher oxygen content. The activity in cyclohexene hydrogenation was very similar for all catalysts prepared by either dry impregnation or wet impregnation (Table 4). Therefore, we selected the DI samples for covering with the protective siliceous coating, because it is more challenging, Pd being located within the pores. In addition, there was a strong effect of the support on the catalytic activity (DG60 > SX+) hence the coverage was only carried out on the most efficient catalysts (supported on DG60) to be able to detect any effect.

Covering on activated carbon supported catalysts

The DI5-DG60 prepared catalyst was covered by a protective siliceous layer before activation by reduction. Textural characterization after covering shows again a great loss in surface area and porosity, demonstrating that an essentially non-porous siliceous layer covers the whole microporous carbon surface. However, thermal treatment at 400 °C restores some surface and pore volume (Table 5). Before covering by the protective layer, the metal dispersion was typically comprised between 10 and 15% for these catalysts. After protection, CO chemisorption gave very low values, indicating complete covering of the active metal. TEM characterization showed small metal nanoparticles (< 10 nm) on DG60 before covering (Fig. 3a). After covering, these Pd particles are embedded under the siliceous coating (Fig. 3b), in agreement with CO chemisorption measurements. XPS characterization of the protected catalysts confirmed covering of Pd by a siliceous layer (Table 6). Indeed, nearly no Pd is detected at the surface, while high amounts of Si, O and N are measured. Some carbon is still being detected but it can originate from organic surface contamination

Table 5 Textural characteristics of catalysts supported on DARCO G60 after covering by a siliceous layer and thermal treatment

Sample	Reduction temperature (°C)	Specific surface area (m^2/g)	Total pore volume (cm^3/g)	Microporous volume (cm^3/g)	Mean pore diameter (Å)	Specific kinetic constant ($M\ min^{-1}\ g_{Pd}^{-1}$)
Si@DI5-DG60	200	30	0.037	0.000	78	0.021
Si@prec-DI5-DG60	200	32	0.024	0.000	65	0.002
Si@DI5-DG60	400	278	0.167	0.068	42	0.021
Si@DI5-SX+	200	30	0.031	0.000	73	0.002
Support SX+	–	981	0.686	0.260	44	–
Support G60	–	954	0.624	0.252	40	–

The cyclohexene hydrogenation activity of the different catalysts is quantified by the specific kinetic constant k′ (solvent = methanol, initial concentration in cyclohexene = 0.6 M, total volume = 0.4 L, m_{Pd} = 4 mg, P_{H_2} = 2 bar, T = 21 °C)

and not only from the exposed support. The sample heated at 400 °C presents more accessible Pd at the surface than the sample heated at 200 °C.

The activity in cyclohexene hydrogenation of the protected catalysts was much lower than for the uncovered ones (Table 5). However, the activity was maintained over days. The loss in activity can be explained by the thick layer of non-porous siliceous coating, as reported in the literature for other types of coatings [28]. This might cause internal diffusional limitations within this layer or diminish the active metal surface available for the reaction to occur. However, by performing the reductive thermal treatment at higher temperature (400 °C), some porosity was restored and accessibility to Pd was regained as described above, and the activity was increased accordingly. TGA-MS study of the covered Si-DI5-DG60 catalyst showed that a mass loss attributable to nitrogen-containing species occurred above 200 °C. XPS also showed the presence of N on the surface, which decreased for the catalyst heated at 400 °C (Table 6). Therefore, we can conclude that it is the degradation of *N*-containing siliceous fragments arising from aminopropyltriethoxysilane that creates the porosity in the cover layer, which is beneficial for the activity.

Investigation of palladium on carbon black catalysts

A third series of experiments were carried out with a covered Pd/CB (CB = carbon black) catalyst that was prepared in one step, i.e. without prior reduction of the catalyst before covering. The content of Pd, Si and carbon in the Pd/CB catalyst covered with siliceous layers was evaluated by X-ray fluorescence spectroscopy and elemental analysis. The Pd loading was 2.10 wt% Pd and the siliceous

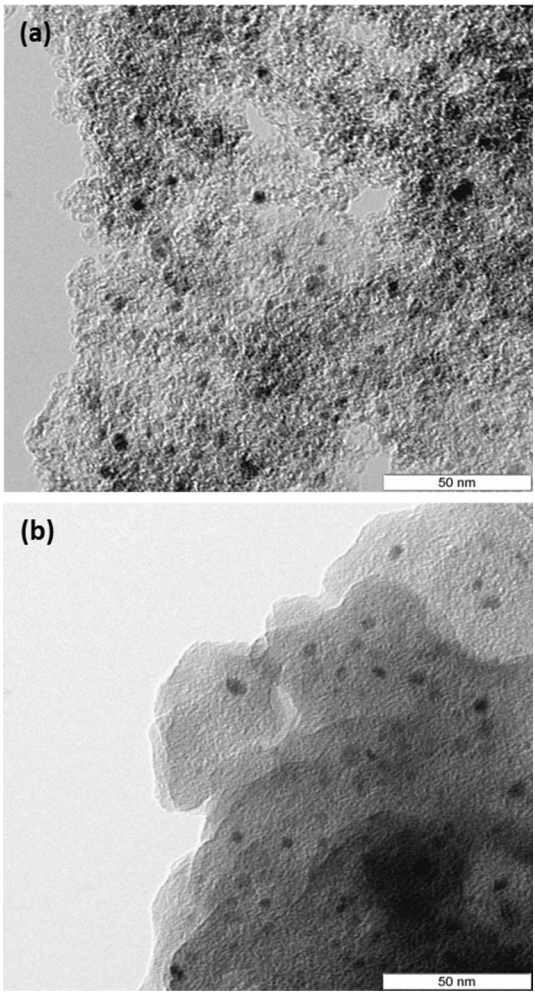

Fig. 3 TEM images of **a** uncovered DI5-DG60 catalyst, **b** protected Si@DI5-DG60 catalyst treated at 200 °C

Table 6 XPS characterization of catalysts prepared on DARCO G60 support and covered by a protecting siliceous layer

Sample	Reduction temperature (°C)	C (%)	O (%)	N (%)	Pd (%)	Si (%)
Si@JM440	–	31.86	40.90	5.08	0.059	21.81
Si@JM440 after reaction	–	37.76	38.13	4.33	0.057	19.55
Si@DI5-DG60	200	36.44	37.83	5.17	0.032	20.20
Si@DI5-DG60	400	36.47	38.44	3.42	0.056	21.48

loading was controlled (here 7 wt%) by adjusting the concentration of TEOS. The Pd particle sizes determined by TEM in the samples with different siliceous loadings after reduction with hydrogen at 200 °C was ~2.0 nm whereas the particle

Table 7 Characterization data of covered carbon black catalyst (7% w/w siliceous layer) treated thermally at 400 and 800 °C

Sample	Reduction temperature (°C)	Specific surface area (m^2/g)	Total pore volume (cm^3/g)	Microporous volume (cm^3/g)	Mean pore diameter (Å)	Metallic Pd dispersion (%)
SiCB7wt-400	400	93	0.783	0.000	328	23
SiCB7wt-800	800	187	0.838	0.037	268	8

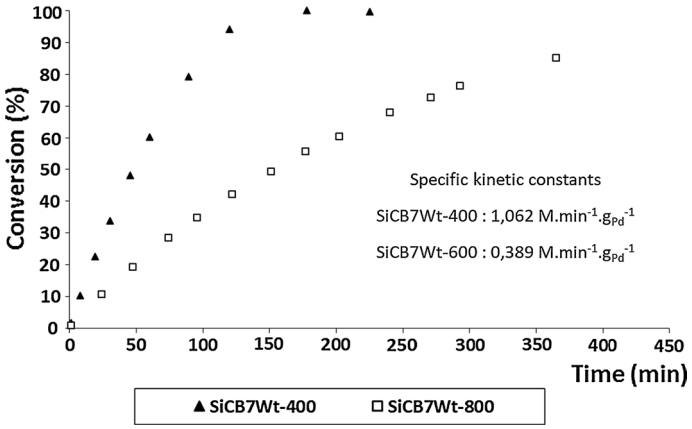

Fig. 4 Cyclohexene conversion versus time for the coated homemade Pd/carbon black catalyst SiCB7wt thermally treated at 400 and 800 °C (reaction conditions: solvent = methanol, initial concentration in cyclohexene = 0.6 M, total volume = 0.4 L, m_{Pd} = 5 mg, P_{H_2} = 2 bar, T = 21 °C)

size of Pd in an uncovered Pd/CB sample prepared similarly in absence of TEOS was 3.7 ± 2.2 nm. The Pd particle sizes were observed by TEM to increase with thermal treatment at higher temperature. However, the values of average Pd diameter in the covered catalyst are smaller (2.5 ± 1.7 nm) than that of uncovered Pd/CB catalyst (5.2 ± 3.8 nm) after heat-treatment at 350 °C. This suggests that the siliceous layer-containing catalysts have a high sintering resistance of their Pd metal particles, thanks to the protecting ability of the covering layers.

The covered Pd/CB catalyst was much more active than those supported on activated carbon described above. This is due to the fact that each carbon support grain being non-porous, the active phase is located on the external surface and remains accessible after coating. This could also be due to a thinner siliceous overlayer using this procedure, as indicated by TEM observations. The protected SiCB7wt catalyst was thermally treated at 400 or 800 °C and the obtained samples were characterized by nitrogen physisorption and CO chemisorption (Table 7). The activity was high in all cases (Fig. 4). By treating at 400 °C, a very active catalyst is obtained, because porosity is created within the siliceous overlayer, as described above. At 800 °C, the catalyst is slightly less active, because the Pd dispersion starts to diminish (see CO chemisorption results in Table 7).

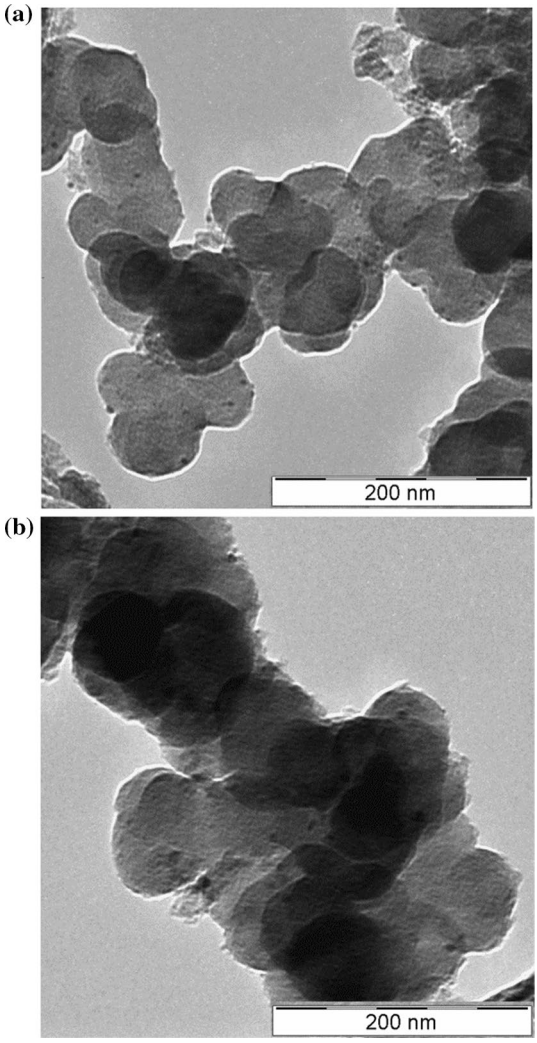

Fig. 5 TEM images of the covered homemade Pd/carbon black catalyst SiCB7wt thermally treated at **a** 400 and **b** 800 °C

This is also visible by TEM (Fig. 5), where the sample treated at 400 °C displays small Pd particles homogeneously dispersed within the support/overlayer matrix. It demonstrates that a compromise has to be found between creating some porosity in the formed siliceous coating and keeping its protecting ability.

However, we have found that in general protecting a Pd/CB catalyst gives better results than when using a microporous carbon support, where the active phase is inserted within the pores. Indeed, in the case of carbon black support, the path towards the active phase is in this case the shortest one, going only through the protecting layer and not through the underlying carbon porosity. The stabilization mechanism of the protecting layer can therefore be viewed as diamond crimping, i.e. each Pd nanoparticle is isolated from its neighboring particles by walls of silica.

This physical barrier avoid metal nanoparticles mobility and merging. The mechanism of protection can therefore be identified here as a mechanical one, rather than playing on the highly complex chemistry of deactivation phenomena.

Conclusion

Industrially-relevant Pd/C catalysts were covered by a microporous siliceous coating in a simple manner. The coated catalysts were characterized by XPS which demonstrated the presence of Si and O, and by electron microscopy which revealed a homogeneous and thick coating. However, the access to the underlying palladium was limited but could (at least partially) be restored by heat-treatment. Indeed, nitrogen-containing groups were thermally removed, which created porosity in the protecting layer. This led to a marked increase in catalytic activity.

In more details, a commercial catalyst was first coated with the protective siliceous layer. By heat-treating at different temperatures, we demonstrated that pores could be created within the thick coating, increasing the catalytic activity thanks to better accessibility to the Pd active phase situated underneath.

Catalysts prepared on microporous activated carbons displayed a stronger loss of activity upon covering. This was especially the case with a catalyst prepared by incipient wetness where we showed that the active phase was situated within the micropores of the carbon support. Sintering was avoided by the coating presence.

The best results were obtained using carbon black as support thanks to the absence of micropores within the carbon grains. This allows the active phase to be situated at the carbon/Si interface and gives rise to highly active catalysts after porosity opening in the coating layer. The mechanism of stabilization against deactivation can be identified as mechanical; where the protecting layer brings physical barriers between the supported Pd particles, hence lowering their mobility and sintering.

Acknowledgements The authors wish to thank the Fonds de la Recherche Scientifique (FRS-FNRS, Belgium) with the assistance of the Fédération Wallonie-Bruxelles and the Belgian National Lottery, as well as the Université catholique de Louvain for funding. We are also grateful to the JSPS (KAKENHI Grant Number 22760599, Japan) for funding. We thank as well Johnson Matthey for the JM440 sample and Grégory Ploegaerts for ICP analyses.

References

1. Blaser H-U, Indolese A, Schnyder A, Steiner H, Studer M (2001) J Mol Catal A 173:3–18
2. Yin L, Liebscher J (2007) Chem Rev 107:133–173
3. Toebes ML, van Dillen JA, de Jong KP (2001) J Mol Catal A 173:75–98
4. Hermans S, Wenkin M, Devillers M (1998) J Mol Catal A 136:59–68
5. Hermans S, Diverchy C, Demoulin O, Dubois V, Gaigneaux EM, Devillers M (2006) J Catal 243:239–251
6. Deffernez A, Hermans S, Devillers M (2007) J Phys Chem C 111:9448–9459
7. Hermans S, Thiltges F, Deffernez A, Devillers M (2012) Catal Lett 142:521–530
8. Willocq C, Dubois V, Khimyak YZ, Devillers M, Hermans S (2012) J Mol Catal A 365:172–180
9. Hermans S, Diverchy C, Dubois V, Devillers M (2014) Appl Catal A 474:263–271

10. Maxted EB (1951) Adv Catal 3:129–178
11. Petró J (1976) In: Szabó ZG, Kalló D (eds) Contact catalysis, vol 2. Elsevier, Amsterdam, pp 65–75
12. Hegedus LL, McCabe RW (1984) Catalyst poisoning. Marcel Dekker, New York
13. Bartholomew CH (2001) Appl Catal A 212:17–60
14. Hegedűs L, Máthé T (2002) Appl Catal A 226:319–322
15. Moulijn JA, van Diepen AE, Kapteijn FF (2008) In: Ertl G, Knözinger H, Schüth F, Weitkamp J (eds) Handbook of heterogeneous catalysis. Wiley, Weinheim, pp 1829–1845
16. Argyle MD, Bartholomew CH (2015) Catalysts 5:145–269
17. Albers P, Pietsch J, Parker SF (2001) J Mol Catal A 173:275–286
18. Moulijn JA, van Diepen AE, Kapteijn F (2001) Appl Catal A 212:3–16
19. Lange J-P (2015) Angew Chem Int Ed 54:13186–13197
20. Sádaba I, López Granados M, Riisager A, Taarning E (2015) Green Chem 17:4133–4145
21. An K, Zhang Q, Alayoglu S, Musselwhite N, Shin J-Y, Somorjai GA (2014) Nano Lett 14:4907–4912
22. Dai Y, Lim B, Yang Y, Cobley CM, Li W, Cho EC, Grayson B, Fanson PT, Campbell CT, Sun Y, Xia Y (2010) Angew Chem Int Ed 49:8165–8168
23. Oh J-G, Oh H-S, Hee Lee W, Kim H (2012) J Mater Chem 22:15215–15220
24. Montini T, Condo AM, Hickey N, Lovey FC, De Rogatis L, Fornasiero P, Graziani M (2007) Appl Catal B 73:84–97
25. Liu H, Zhang L, Wang N, Sheng SuD (2014) Angew Chem Int Ed 53:12634–12638
26. Zhang C, Zhou Y, Zhang Y, Zhang Z, Xu Y, Wang Q (2015) Powder Technol 284:387–395
27. Zhang N, Xu Y-J (2013) Chem Mater 25:1979–1988
28. Comandella D, Woszidlo S, Georgi A, Kopinke F-D, Mackenzie K (2016) Appl Catal B 186:204–211
29. Simescu-Lazar F, Meille V, Pallier S, Chaînet E, De Bellefon C (2013) Appl Catal A 453:28–33
30. Takenaka S, Matsumori H, Nakagawa K, Matsune H, Tanabe E, Kishida M (2007) J Phys Chem C 111:15133–15136
31. Nakagawa K, Tanimoto Y, Sotawa K, Sugiyama S, Takenaka S, Kishida M (2009) Chem Lett 38:480–481
32. Nakagawa K, Tanimoto Y, Okayama T, Sotowa K, Sugiyama S, Moriga T (2010) Stud Surf Sci Catal 175:201–208
33. Nakagawa K, Tanimoto Y, Okayama T, Sotowa K, Sugiyama S, Takenaka S, Kishida M (2010) Catal Lett 136:71–76
34. Nakagawa K, Okayama T, Tanimoto Y, Sotowa K, Sugiyama S, Moriga T, Takenaka S, Mishida M (2012) Appl Catal A 13:419–420
35. Dubois V, Jannes G (2013) Appl Catal A 468:459–466
36. Dubois V, Jannes G, Verhasselt P (1997) Stud Surf Sci Catal 108:263–271
37. Lemaitre JL, Menon PG, Delannay F (1984) The measurement of catalyst dispersion. In: Delannay F (ed) Characterization of heterogenous catalysts. Marcel Dekker, New York
38. Krishnankutty N, Vannice MA (1995) J Catal 155:312–326
39. Dubois V, Dal Y, Jannes G (2002) Stud Surf Sci Catal 143:993–1002